PNAS Nexus, 2024, 3, pgae536
https://doi.org/10.1093/pnasnexus/pgae536
Advance access publication 25 November 2024
Research Report

Insights into the regulation of CHIP E3 ligase-mediated ubiquitination of neuronal protein BNIP-H

Srihari Shankar[a], Yaochen Liu[a], Nikhil Kumar Tulsian[a,1], Boon C. Low[a,b,c], Qingsong Lin[a] and J. Sivaraman[a,*]

[a]Department of Biological Sciences, National University of Singapore, Singapore 117543
[b]Mechanobiology Institute, National University of Singapore, Singapore 117411
[c]NUS College, National University of Singapore, Singapore 138593
[1]Present address: MSD International GmbH, 8 Biomedical Grove, Neuros, Singapore 138665
*To whom correspondence should be addressed: Email: dbsjayar@nus.edu.sg
Edited By Nancy Bonini

Abstract

BCL2/adenovirus E1B 19-kDa protein-interacting protein 2 homolog (BNIP-H or Caytaxin), a pivotal adaptor protein that facilitates cerebellar cortex growth and synaptic transmission, is posttranslationally modified to regulate neuronal function. This study reports the ubiquitination of BNIP-H by Carboxyl terminus of Hsc70-Interacting Protein (CHIP), a U-box containing E3 ligase that is also regulated *via* autoubiquitination. Specifically, it was observed that CHIP autoubiquitinated itself primarily at Lys23 and Lys31 *in vitro*. Mutation of these residues shows the autoubiquitination of successive lysines of CHIP. In total, nine lysines on CHIP were identified as the autoubiquitination sites, the collective mutation of which almost completely terminated its autoubiquitination. Additionally, CHIP-mediated ubiquitination of BNIP-H is completely inhibited when BNIP-H bears arginine mutations at four key lysine residues. Next, using hydrogen deuterium exchange mass spectrometry, a model of a plausible mechanism was proposed. The model suggests transient N-terminal interactions between the CHIP and BNIP-H which allows for the swinging of U-box domain of CHIP to ubiquitinate BNIP-H. Following complex dissociation, BNIP-H population is regulated *via* the ubiquitin-proteasome pathway. Collectively, these results aid in our understanding of CHIP-mediated BNIP-H ubiquitination and provide further insight into the roles of these proteins in neuritogenesis and neurotransmission.

Keywords: E3 ligase, ubiquitination, HDX-MS, neuron, BCH-domain

Significance Statement

This study elucidates the critical interaction between the adaptor protein BCL2/adenovirus E1B 19-kDa protein-interacting protein 2 homolog (BNIP-H) and the E3 ligase Carboxyl terminus of Hsc70-Interacting Protein (CHIP), highlighting their essential roles in brain development and neuronal function. Through detailed mapping and mutational analysis, we identify key lysine amino acids involved in the autoubiquitination of CHIP and ubiquitination of BNIP-H, revealing the insights into their regulation in the cells. The findings demonstrate that the ability of CHIP to ubiquitinate BNIP-H is significantly impeded when key lysines in BNIP-H are mutated, underscoring the specificity of this interaction. Furthermore, hydrogen–deuterium exchange mass spectrometry analysis suggests a model where transient N-terminal domain interactions facilitate CHIP's U-box-mediated ubiquitination of BNIP-H. These insights advance our understanding of how BNIP-H and CHIP contribute to neuronal physiology and brain development.

Introduction

BCL2/adenovirus E1B 19-kDa protein-interacting protein 2 homolog (BNIP-H), also known as Caytaxin, belongs to the BCL2/adenovirus E1B 19-kDa protein-interacting protein-2 (BNIP-2) family (1). When dysfunctional, this crucial protein leads to a neurodegenerative disease called Cayman-type cerebellar ataxia, a disorder characterized by hypotonia, variable psychomotor retardation, and cerebellar dysfunction (2). BNIP-H behaves as an adaptor protein, facilitating the transport of cargo, such as adenosine triphosphate (ATP) citrate lyase and kidney-type glutaminase, to support neuronal development (3, 4). Additionally, BNIP-H tethers to and similarly transports mitochondria (5). Numerous metabolic and enzymatic pathways rely on BNIP-H regulation; albeit its precise mechanism of action is largely unclear.

BNIP-H regulation involves various mechanisms, including ubiquitination, a posttranslational modification that marks the protein for proteolytic degradation (6). Ubiquitination involves a myriad of proteins: E1 ubiquitin-activating enzyme, E2 ubiquitin-conjugating enzyme, E3 ubiquitin ligase, ubiquitin, and a substrate protein (7, 8). CHIP (carboxyl terminus of Hsc70-Interacting Protein), a U-box

Competing Interests: The authors declare no competing interests.
Received: May 8, 2024. **Accepted:** November 4, 2024

containing E3 ligase, acts both as a co-chaperone to assist with the refolding of misfolded proteins and as an E3 ligase that targets misfolded proteins for degradation through the proteasomal pathway (9). CHIP dysregulation has been linked to neurodegenerative diseases, such as Alzheimer's disease and Parkinson's disease (10), with mutations in CHIP leading to ataxia. In contrast, its overexpression offers neuroprotectivity against various neurological diseases (10).

CHIP contains three conserved tetratricopeptide repeats (TPR) each of 34-amino acids for protein–protein interactions (9) and a U-box domain for ligase activity. Although CHIP is known to ubiquitinate neuronal proteins (6), the exact mechanism by which the substrates are recognized and regulated by CHIP remains elusive. One particular target, BNIP-H, is critical in learning and memory, with its excessive degradation leading to impaired function (11). Thus, there is a critical need to understand the regulatory role of BNIP-H more clearly.

In this study, we present a comprehensive analysis of the autoubiquitination of the mouse CHIP E3 ligase and the ubiquitination of its substrate, mouse BNIP-H. In CHIP, we identified nine lysine residues that are involved in its autoubiquitination. Further, through *in vitro* analyses, we identified four lysine residues that are crucial for the ubiquitination of BNIP-H by CHIP. Finally, we mapped the interaction of BNIP-H and CHIP using hydrogen–deuterium exchange mass spectrometry (HDX-MS) and proposed a model to describe the mechanism of regulation of the substrate by the E3 ligase. Overall, our findings provide evidence for the mode of CHIP-mediated ubiquitination of BNIP-H and offer further insight into the possible roles of CHIP and BNIP-H in neuronal development.

Results

Autoubiquitination of CHIP at Lys23 and Lys31

The active CHIP E3 ligase is regulated in various ways, including autoubiquitination *via* its U-box domain (12). We observed that the purified wild-type (WT) CHIP E3 ligase ($CHIP^{WT}$) undergoes autoubiquitination in the presence of purified E1 (Ube1) and E2 (UbcH5B) enzymes (Fig. 1A–C). Through mass spectrometry (MS) analysis, we found that CHIP is ubiquitinated at two lysine residues: Lys23 and Lys31 (Supplementary Fig. S1). In MS analysis, ubiquitination sites are identified by a 114.04 Da mass shift in tryptic peptides, corresponding to a diglycine remnant in MS/MS spectra. However, iodoacetamide, a common alkylating agent in protein digestion protocols, can generate 2-acetamidoacetamide, which has an identical molecular mass to the diglycine adduct, potentially leading to false positive identifications (13–15). To clarify and validate the importance of these residues in autoubiquitination, we generated single Lys23Arg and Lys31Arg mutants as well as a Lys23,31Arg double-mutant protein and performed ubiquitination assays. We observed reduction in the level of autoubiquitination species for the Lys23Arg (33%), Lys31Arg (17%), and Lys23,31Arg double mutant (36%), affirming the key roles of these lysines in the ubiquitination process (Fig. 1C). While previous reports suggest that these lysine residues are essential for CHIP autoubiquitination (16, 17), our single and double mutants indicated that these residues were not indispensable to the autoubiquitination process (Fig. 1B). The lack of complete termination of autoubiquitinated CHIP species (Fig. 1C) in the Lys23,31Arg double mutant suggests that these residues are the first to be autoubiquitinated and, their absence triggers the initial ubiquitination to shift to other lysine residues, particularly since polyubiquitination remains intact.

Autoubiquitination of CHIP at other lysines

We next sought to assess the potential roles of other lysine residues in CHIP autoubiquitination. Previous studies have indicated that Ube2W-CHIP (E2-E3 enzymes) facilitates autoubiquitination at the N-terminus of CHIP, consisting of lysines at positions 2, 4, and 7 (18, 19). Thus, we investigated the role of this lysine-rich N-terminus by generating a Lys2,4,7Arg triple mutant (Supplementary Fig. S2A). Furthermore Windheim et al. identified polyubiquitination of Lys221 and Lys255 (in human CHIP) in the presence of UbcH5a *in vitro* (16). Thus, we also generated a Lys222,256Arg CHIP double mutant (equivalent to 221 and 255 lysines in human isoform). Finally, we generated a CHIP mutant bearing all seven arginine substitutions (henceforth referred as $CHIP^{7M}$) (Supplementary Fig. S1B).

Antiubiquitin blot showed a similar formation of polyubiquitin chains among the WT and all mutant CHIP proteins (Fig. 1D and E). The level of autoubiquitination for the Lys222,256Arg mutant was similar to that of $CHIP^{WT}$ (<10% difference), suggesting that these residues are not primarily involved in its autoubiquitination. In contrast, there was a significant reduction (39.5%) in the degree of ubiquitination for the Lys2,4,7Arg triple mutant as compared with $CHIP^{WT}$, indicating that these residues have a more key role. As anticipated, the $CHIP^{7M}$ mutant displayed the lowest degree of (48.5%) autoubiquitination, implying an additive effect of the mutations on CHIP autoubiquitination (Fig. 1F). However, since the ubiquitination of CHIP was not completely inhibited, it stands to reason that other lysine residues could be playing a compensatory role.

Through MS analysis (in-gel digestion) of the protein bands corresponding to ubiquitinated $CHIP^{7M}$ mutant (Fig. 1E), we identified additional two lysine residues bearing ubiquitination marks: Lys42 and Lys126. Thus, we generated single-point mutants of these residues (Lys42Arg and Lys126Arg CHIP mutants) as well as a mutant bearing nine substitutions ($CHIP^{9M}$; Lys2,4,7,23,31,42,126,222,256Arg). Ubiquitination assays using the $CHIP^{WT}$ and single-mutant CHIP (Lys42Arg and Lys126Arg) proteins showed that polyubiquitin formation was not impeded (<10% difference) by either of these mutations (Fig. 1H), suggesting that E3 ligase activity was not hampered. Each of the single mutations displayed autoubiquitination levels similar to that of $CHIP^{WT}$, suggesting that these residues are not the primary lysine residues responsible for autoubiquitination. Intriguingly, the $CHIP^{9M}$ mutant showed a massive decrease (81%) in the levels of autoubiquitination, indicating that, by this point, we had identified most of the crucial lysine residues involved in CHIP autoubiquitination (Fig. 1I).

Despite these nine mutations, the $CHIP^{WT}$ and $CHIP^{9M}$ mutant proteins showed similar elution profiles in gel filtration chromatogram (Supplementary Fig. S2D), and no differences were detected in the circular dichroism (CD) spectra (Supplementary Fig. S2E). This highlights that the WT and mutant proteins are similar in their structural properties and observed differences in the ubiquitination profiles are likely associated with the loss of free amines in the lysine residues. Notably, although mostly inhibited, there remains minute autoubiquitination activity in the $CHIP^{9M}$ mutant (Fig. 1I). Any additional residues were unable to be identified by MS, due to the very low levels of autoubiquitination in the $CHIP^{9M}$ mutant.

The CHIP structure (PDB 2C2L (20)) shows an even distribution of these nine key lysine residues across the surface-exposed regions of the protein. Overall, CHIP comprises 20 lysine residues and, drawing insight from literature and our results, we can define the role of nine of these lysine residues in autoubiquitination.

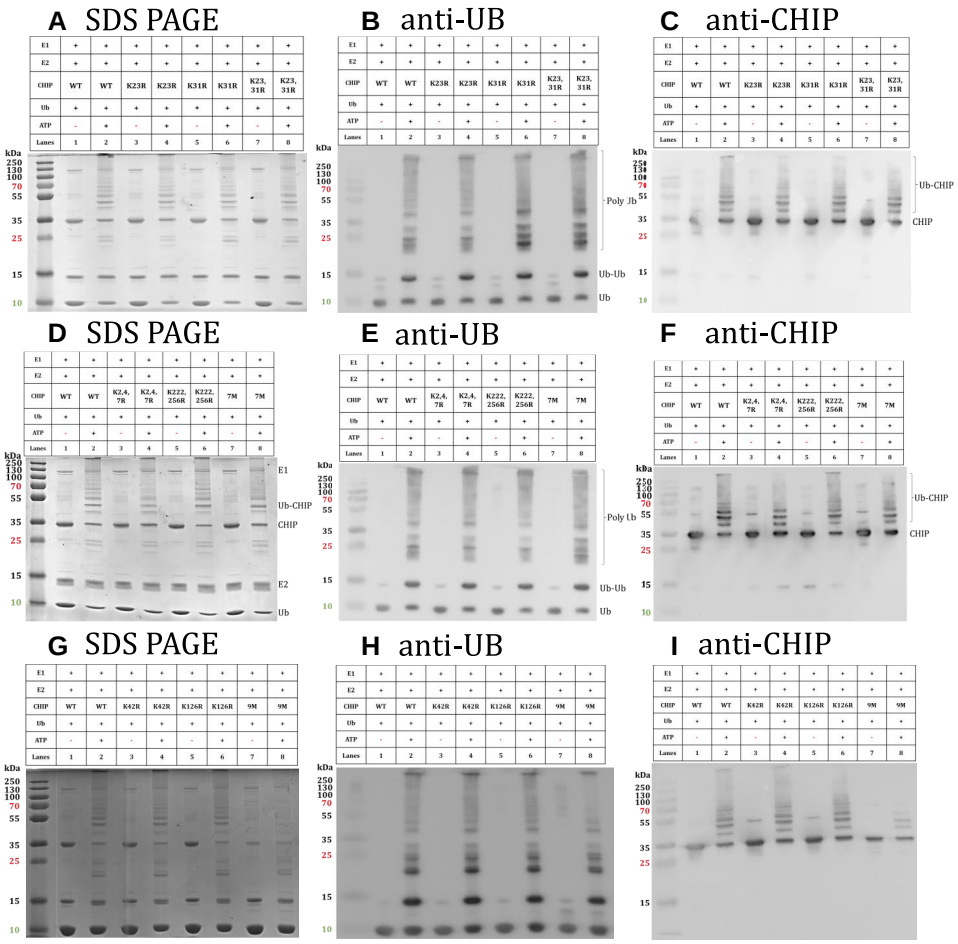

Fig. 1. Autoubiquitination of CHIP and its mutants. The SDS PAGE, anti-UB and anti-CHIP are shown for CHIP mutants A–C) WT, K23R, K31R, and K23,31R that shows reduction in the double mutant (K23,31R). Lane 8 shows that autoubiquitination still exists through the ubiquitination of other residues. D–F) WT, K2,4,7R, K222,256R, and 7M (K2,4,7,23,31,222,256R) where K2,4,7R and 7M show the lowest autoubiquitinations. G–I) WT, K42R, K126R, and 9M indicates that the autoubiquitination almost ceases in the 9M mutant that suggests that all crucial lysines that are prone to ubiquitination are identified.

Among these, two (Lys222 and Lys256) out of nine are located in the U-box domain, and three (Lys31, Lys42, and Lys126) are present in the TPR regions (Supplementary Fig. S2A–C).

BNIP-H ubiquitination by CHIP occurs on surface exposed lysines

BNIP-H (Caytaxin) is a 42-kDa (aa1-371) acidic neuroprotective protein consisting of a C-terminal **B**NIP2 and a **C**dc42 **h**omology (BCH) domain, a domain that is known to be structurally complex (21, 22). The mouse variant closely resembles the human homolog (Supplementary Fig. S3A). *In vitro* ubiquitination assays were conducted with purified BNIP-H, CHIP (E3), UbE1 (E1), UbcH5b (E2), and ubiquitin proteins, with and without ATP. Through these assays, we observed BNIP-H to be polyubiquitinated in the presence of CHIP (Fig. 2), confirming that BNIP-H is a substrate of the E3 ligase, as briefly observed in a previous study (6). Moreover, CHIP undergoes autoubiquitination regardless of the presence of BNIP-H (Fig. 2B and D).

BNIP-H is crucial in neuronal function; thus, its ubiquitination by CHIP and subsequent proteasomal degradation ought to be tightly regulated. To identify which lysine(s) on BNIP-H are ubiquitinated, the bands corresponding to ubiquitinated BNIP-H (Fig. 2A) from denatured polyacrylamide electrophoresis were excised and analyzed through MS. We identified BNIP-H ubiquitination on lysine residues 61, 128, 291, and 350 (Supplementary Fig. S1). Thus, we created single mutants for each of these residues, as well as one quadruple mutant (BNIP^{4M}; Lys61,128,291,350Arg). Ubiquitination was retained for each of the single mutants, suggesting that the other three lysine residues in each mutant compensated for the loss of activity of the mutated residue (Fig. 3). BNIP-H ubiquitination was almost completely inhibited (95% reduction in ubiquitination) in the BNIP^{4M} mutant (Supplementary Fig. 3C), confirming the indispensable role of these specific four lysine residues. Additionally, it is well known that CHIP can promote many types of lysine linked (lysine 27, 48, or 63) ubiquitin chains to control its substrates in cells (9, 15, 20, 23). Our MS results primarily show the presence of Lys48 linked chains (Supplementary Fig. S1) on BNIP-H which is the specific ubiquitin modification that is often related to proteasomal degradation (24, 25).

To rule out the possibility that the loss of ubiquitination on the BNIP^{4M} was due to misfolding, CD experiments were performed comparing BNIP^{WT} and all BNIP-H mutants. Similar CD spectra were obtained for all proteins tested (Supplementary Fig. S3D), suggesting that the mutations do not alter the global structure of the protein. Additionally, time-point based assays showed that the BNIP^{4M} mutant is ubiquitinated at a much lower rate than the

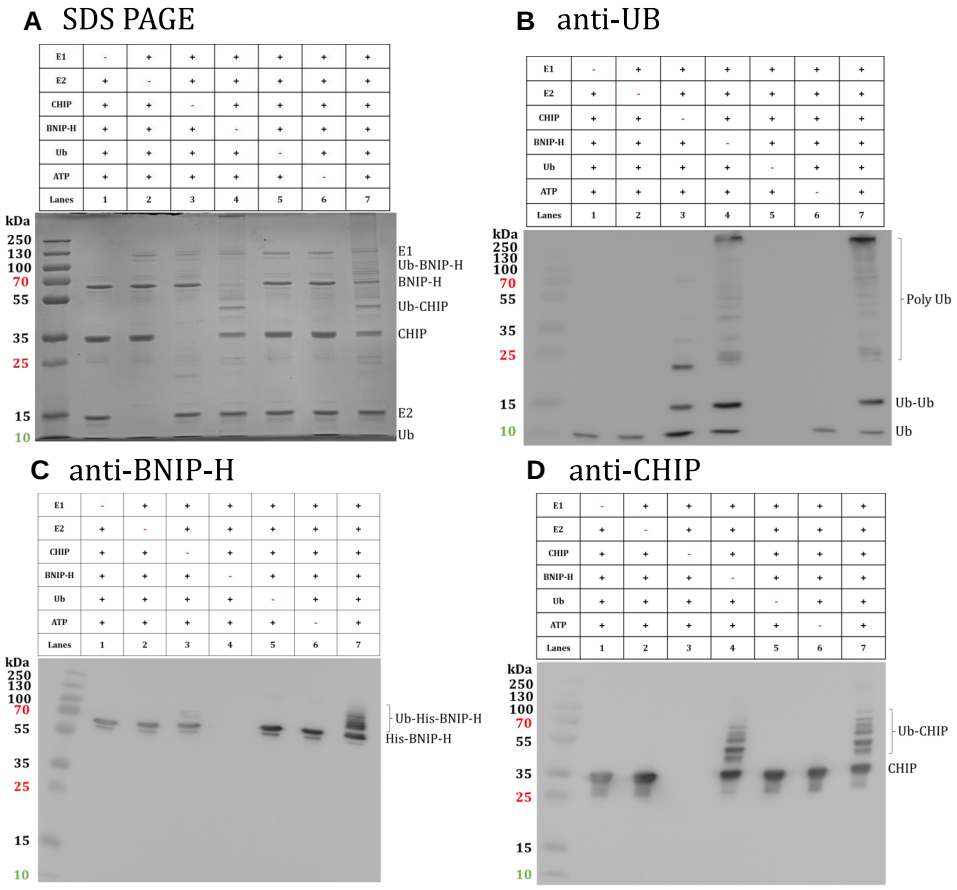

Fig. 2. BNIP-H is ubiquitinated by CHIP E3 ligase. A) SDS page gel shows the ubiquitination reactions with lanes 1–6, each with one missing component. The ubiquitination of BNIP occurs only in the presence of E1, E2, CHIP E3, Ub, and ATP as seen in lane 7. B) Anti-UB blot shows the formation of polyubiquitin chains in lanes 4 and 7. C) Anti-BNIP blot indicates the polyubiquitination of BNIP occurring strongly in the presence of CHIP E3 ligase. D) Anti-CHIP blot shows its autoubiquitination in the presence of ATP in lanes 4 and 7.

BNIP^{WT} protein under identical conditions (Supplementary Fig. S4). This further validates that the loss of ubiquitination in the mutants is due to the loss of free amines. The lysine residues are located on the surface of the protein where they can be accessed and ubiquitinated by CHIP E3 ligase (Supplementary Fig. S3C).

To summarize, while CHIP^{WT} was largely incapable of ubiquitinating BNIP-H^{4M}, the CHIP^{9M} mutant was able to ubiquitinate BNIP-H^{WT}, although not as effectively as CHIP^{WT} (Fig. 3C).

Mapping the interaction interface regions between BNIP-H and CHIP proteins using HDX-MS

We employed HDX-MS to delve deeper into the interaction between CHIP and BNIP-H, with incubation periods similar to the ubiquitination assay. In the presence of the BNIP-H^{WT} substrate, there were marginal changes in deuterium exchange across CHIP^{WT}, particularly within the peptides spanning the TPR and U-box (Fig. 4A) regions. These marginal changes in the deuterium exchange values indicate shielding of the folded regions from the surrounding deuterium, with very slow exchange kinetics. The TPR domain is involved in complex formation with other CHIP substrates, such as Hsc70 and Hsp90 (26, 27), presumably to stabilize the CHIP^{WT}/BNIP-H^{WT} complex for ubiquitination. Mapping of deuterium exchange data onto a full-length model structure of CHIP^{WT}, highlighted these conformational changes across the TPR domain and U-box to be colocalized spatially. Interestingly, when bound to CHIP^{WT}, BNIP-H^{WT} exhibited a global decrease in deuterium exchange across the protein, suggesting that these regions have reduced solvent accessibility, as might be observed as a result of its interaction with CHIP (Fig. 4B). Importantly, decreased deuterium exchange was observed in peptides that spanned the N-terminus and BCH domain of BNIP-H^{WT} (Fig. 4B). Additionally, it is predicted that the region spanning amino acids 1–60 of BNIP-H is highly disordered or unfolded and exposed (Supplementary Fig. S3C), and likely gains a stable secondary structure upon binding to CHIP, as indicated by reduced exchange in that region in the presence of the E3 ligase CHIP. Multiple peptides spanning residues 110–120 aa of BNIP-H showed significantly lower deuterium uptake, suggesting that this region interacts with the TPR domain of CHIP. This corroborates the findings of previous reports that indicated that this region interacts with the TPR domain of kinesin light chain (3, 5). We verified the interaction between a structurally similar TPR domain and a BNIP-H peptide using Isothermal titration calorimetry (ITC) that validates our HDX-MS results (Supplementary Fig. S3E). Collectively, these results suggest that, in the CHIP^{WT}/BNIP-H^{WT} complex, BNIP-H undergoes substantial decreases in deuterium exchange, indicative of a global conformational change.

HDX-MS analyses were additionally carried out for the CHIP^{9M} and BNIP-H^{4M} mutant proteins. The results showed short-term (1 and 10 min) intrinsic dynamic changes in CHIP^{9M}. These changes were localized to the three TPR regions spanning residues 25–128, with a few additional changes recorded in the U-box domain (Fig. 4C). Deuterium exchange kinetics of BNIP-H^{4M} showed

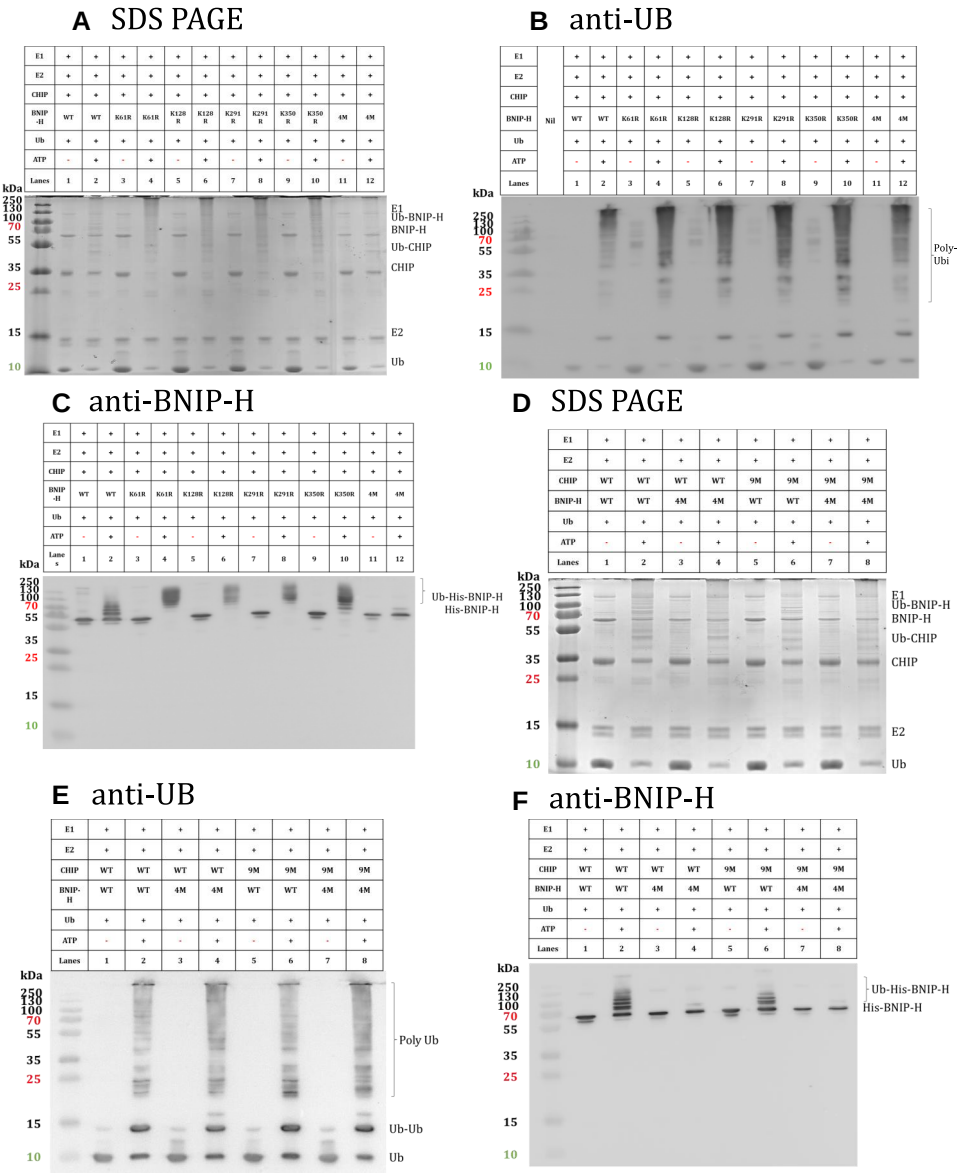

Fig. 3. Ubiquitination of WT and mutant BNIP-H by WT and mutant CHIP E3 ligase. A–C) The mutant proteins K61R, K128R, K291R, K350R, and 4M (K61R,128,291,350R) by CHIP^{WT}. The anti-BNIP shows the 4M mutant is no longer ubiquitinated by CHIP E3 ligase indicating the loss of all crucial lysines. D–F) Ubiquitination assays involving BNIP-H^{WT} and BNIP-H^{4M} mutant with CHIP^{WT} and CHIP^{9M} mutant. The best ubiquitination of BNIP-H occurs in the presence of WT CHIP (lane 2). CHIP^{9M} mutant is still capable of ubiquitinating BNIP-H^{WT} albeit to a much lesser extent (29% reduction) (lane 6). BNIP-H^{4M} mutant shows almost complete termination (95% reduction) in ubiquitination in the presence of CHIP^{WT} as well as CHIP^{9M}. All polyubiquitin chains are formed normally in the anti-Ub blots.

consistently lower exchange for two peptides: 9–34 and 117–137 (Fig. 4D). These changes corresponded with those observed for the BNIP-H^{WT} protein, as these regions interact with CHIP^{9M}. Notably, our results are consistent with previous studies showing that acidic regions around ^{19}WQ^{20} and ^{118}WED^{120} facilitate interactions with the TPR domains of motor proteins (3, 5, 28, 29).

We further observed prominent HDX changes for CHIP^{9M} complexed with BNIP-H^{4M}, suggesting that this complex is sustained longer than their WT counterparts (Fig. 4E); this is because the mutant CHIP^{9M}/BNIP-H^{4M} complex has a delayed dissociation due to the reduced ubiquitination efficiency CHIP for the substrate (Supplementary Fig. S4). Taken together, our HDX-MS results for the WT and mutant proteins complement those from our ubiquitination assays. Collectively, our results allowed us to propose a model for the CHIP^{WT}/BNIP-H^{WT} complex interaction (Fig. 5).

Discussion

Ubiquitination plays a crucial role in the regulation of active proteins in cells by targeting misfolded, partially folded, or unfolded proteins for degradation in the proteasome. Consequently, mutations in proteins involved with directing the ubiquitination process can have disastrous effects on the cell and lead to various diseases and disorders (30). Previous studies have elucidated the role of ubiquitination on the function and turnover of the CHIP E3 ligase (16, 17, 19, 31). While one report has shown that BNIP-H ubiquitination occurs through CHIP (6), the involved residues and its mode of ubiquitination are not understood. Our studies reported here identified the residues involved in the ubiquitination and further provides molecular basis of the autoubiquitination of CHIP E3 ligase, which is known to be relevant in influencing its dimerization, thereby directly impacting its activity

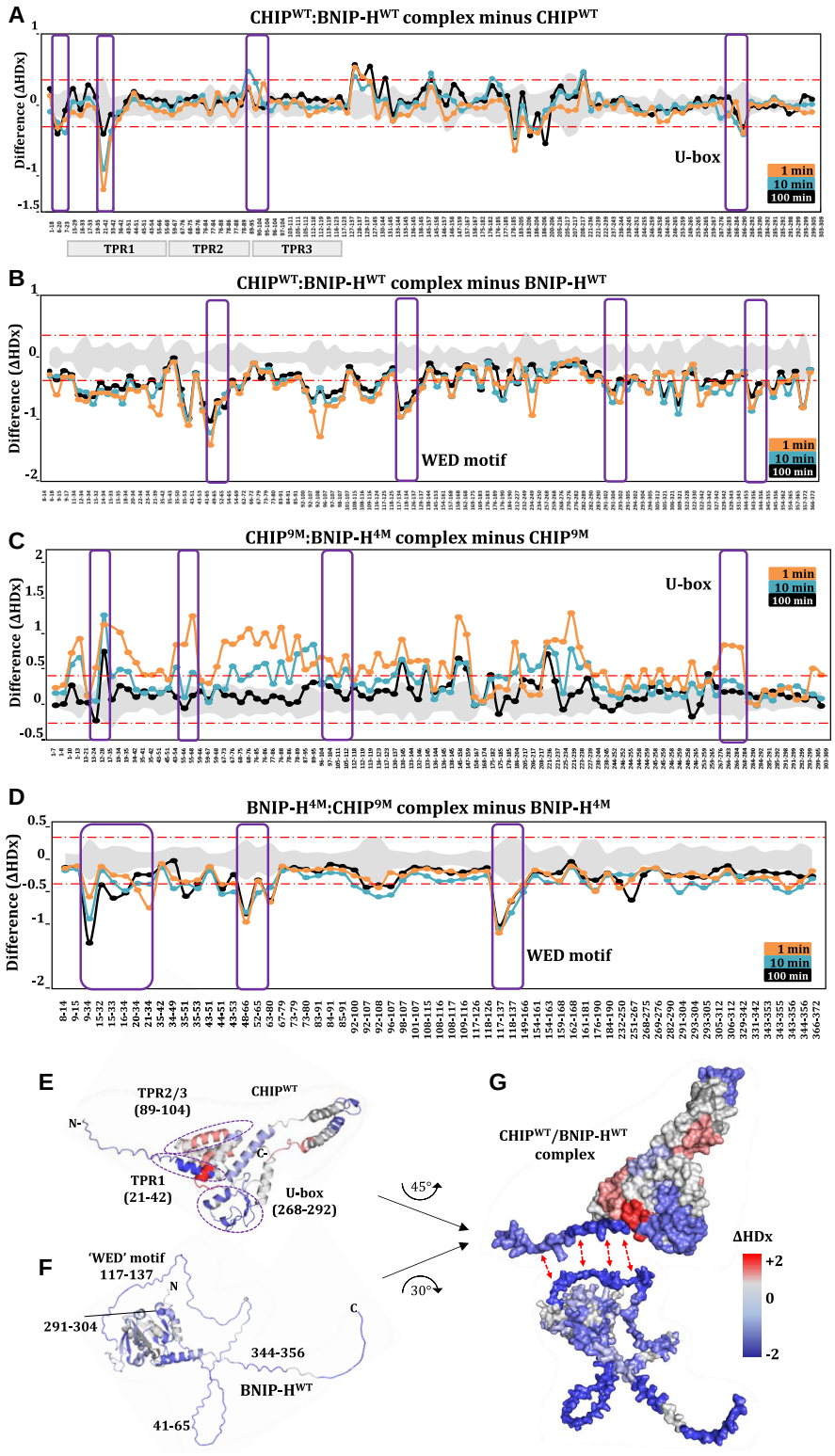

Fig. 4. HDX-MS of WT and mutant BNIP-H and CHIP. Plots showing differences in deuterium uptake (Y-axis) across three deuterium labeling timepoints for CHIP^{WT}-BNIP-H^{WT} complex in comparison with A) free CHIP^{WT} and B) BNIP-H^{WT} apo proteins. Residue numbers of various peptide fragments of A) CHIP^{WT} and B) BNIP-H^{WT} are indicated on X-axis. Average deuterium exchange values are plotted, with standard errors are shaded. A significance threshold (±0.3 D) based on 99% confidence is considered and indicated by dashed lines. Key regions showing decreased deuterium uptake are highlighted in boxes. Plots showing differences in deuterium exchange between the complexed vs. free mutant proteins C) CHIP^{9M} and D) BNIP-H^{4M} are depicted at various labeling time points. The residue numbers for each peptide are indicated. E) Differences at 1 min labeling time are mapped onto dimeric structure of CHIP^{WT}, as indicated with peptides spanning 21–42 (TPR1), 89–104 (TPR2/3) and U-box (268–292) highlighted. F) Differences at 1 min labeling time are mapped onto predicted model of BNIP-H^{WT} (AF-Q86WG3-F1), shown in cartoon representation. Peptides 41–65, 117–137, 291–302, and 344–356 are indicated. G) A model of CHIP^{WT}-BNIP-H^{WT} complex is shown in surface representation, with the TPR regions of CHIP^{WT} (top) interacting with the region spanning the WED motif of BNIP-H^{WT} (bottom).

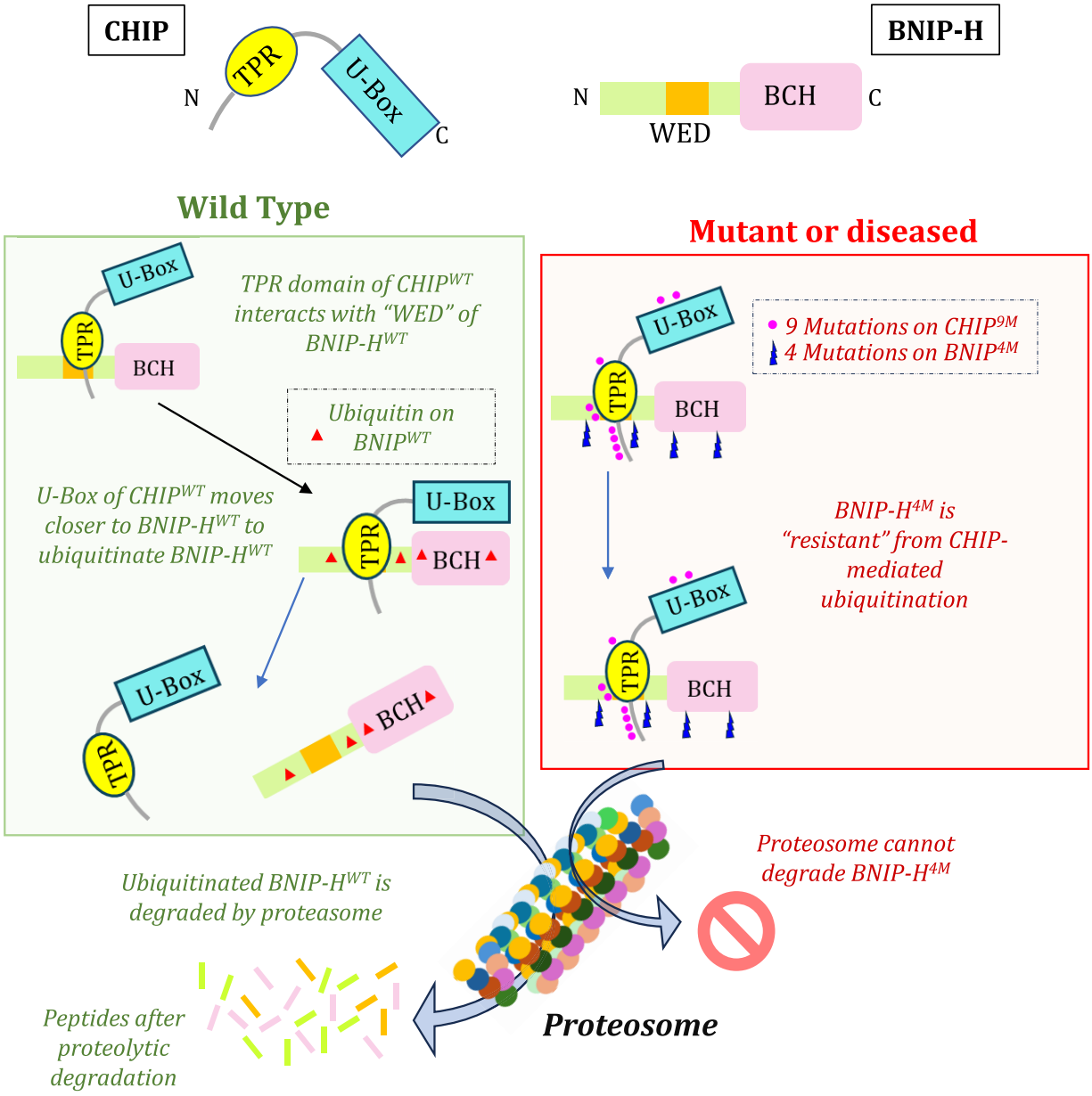

Fig. 5. Proposed model of CHIP-mediated ubiquitination of substrate BNIP-H. The CHIP E3 ligase has the TPR domain and the C terminal U-box domain. The BNIP-H protein consists of the N-terminal region and the C terminal BCH domain. The binding between WT proteins BNIP-H and CHIP is likely to be initiated by the TPR domain (on CHIP) as it binds to the WED motif (^{110}GNGNELEWEDD^{120} in BNIP-H). This allows for the U-box domain to move closer and add ubiquitin on the Lysines 61, 128, 291, and 350 of the substrate BNIP-H. This ubiquitination occurs successfully in the case of WT proteins (as shown by four triangles on BNIP-H^{WT}). Mutant proteins are indicated with nine dots on CHIP^{9M} (corresponding to the nine mutations) and four bolts on BNIP-H^{4M}. These proteins lack the crucial lysines required for ubiquitination. In the mutants, the lack of these four lysines no longer makes BNIP-H a substrate for CHIP and therefore CHIP is incapable of ubiquitinating it. Hence, in the WT proteins, BNIP-H^{WT} is ubiquitinated and degraded by the proteosome in a CHIP-mediated manner while this regulation possibly drastically ceases in the mutant variants. Therefore, proper facilitation of BNIP-H population occurs in the case of WT proteins while the mutant proteins will undergo dysregulation followed by diseased phenotypes.

(17). This autoubiquitination is known to disrupt the binding of CHIP to chaperones, which are protein-folding complexes that are upregulated during cellular stress (17).

In this study, we found that four crucial lysine residues in BNIP-H are ubiquitinated by CHIP, and that CHIP itself is autoubiquitinated *via* nine lysine residues, thus highlighting the regulation of this U-box containing E3 ligase. Lam et al. and Thrower et al. had proposed that lengthened polyubiquitin chains allow for increased retention of substrate proteins at the proteasome due to slower deubiquitination of the longer polyubiquitin chains (32, 33). Our findings are in support of this theory, as lysine single-point mutants of BNIP-H exhibited only reduced ubiquitination rather than complete inhibition of function, with compensation presumably achieved by the remaining three essential lysine residues. Furthermore, the mutant BNIP-H would be unavailable to participate in its usual cellular functions by being retained in the proteosome. This mechanism is possible physiologically, as the accumulation of mutated BNIP-H could disrupt proper cellular function.

Table 1. Summary of key amino acids known from prior findings with current advances present in this study.

Protein	Mutant	Findings compared with WT protein	Reference
CHIP E3 Ligase (mouse)			
CHIP	K23R	K23 is shown to be ubiquitinated. K23R mutant protein shows slightly reduced autoubiquitination.	Equivalent K22 in human CHIP found to be monoubiquitinated (16) and this study
CHIP	K31R	K31 is also shown to be ubiquitinated. K31R mutant protein shows slightly reduced autoubiquitination	Equivalent lysine in human found to be ubiquitinated (17) and this study
CHIP	K23,31R	Double mutant shows slightly reduced autoubiquitination	This study
CHIP	K2,4,7R	K2,4,7R shows reduced autoubiquitination	K2 is important for CHIP's function (31) and this study
CHIP	K222,256R	K222, 256R shows similar autoubiquitination	K221, 255 in human identified to be polyubiquitinated (16) and this study
CHIP	7M	Drastically reduced autoubiquitination. Monoubiquitination band still observed.	This study
CHIP	K42R	K42 is ubiquitinated. K42R shows almost no change in autoubiquitination which suggest it is not primary lysine to be targeted	This study
CHIP	K126R	K126 is ubiquitinated. K126R almost no change in autoubiquitination which suggest it is not primary lysine to be targeted	This study
CHIP	9M	Almost completely abolished autoubiquitination	This study
BNIP-H (mouse)			
BNIP	K61R	Mutant undergoes heavier polyubiquitination	This study
BNIP	K128R	Mutant undergoes heavier polyubiquitination. Slightly fainter bands compared with rest of the mutants	This study
BNIP	K291R	Mutant undergoes heavier polyubiquitination	This study
BNIP	K350R	Mutant undergoes heavier polyubiquitination	This study
BNIP	4M	Abolishes polyubiquitination	This study

Our results, along with supporting literature, allow us to propose that WT CHIP and its BNIP-H substrate interact transiently at their N-terminal domains; more specifically, between the TPR of CHIP and the "WED" motif of BNIP-H. This interaction might allow the U-box of CHIP to swing and ubiquitinate any of the four crucial lysines of BNIP-H (Fig. 5, Table 1) followed by dissociation of the complex. This is a representative mechanism of CHIP substrate regulation. Moreover, previous studies show that such acidic peptide regions can interact with the TPR regions (structurally similar to the TPR regions of CHIP E3 ligase) kinesin motor proteins to carry-out cargo transport (3, 5, 29) which is in agreement with our study and validates that TPR forms a docking platform for BNIP-H for different functions. Of note, our research highlights the regulation of BNIP-H by CHIP in relation to the E2 enzyme, UbcH5b. Other reports indicate notable differences in ubiquitination outcomes for CHIP substrates like Hsp70 and ataxin-3 depending on the interacting E2 enzyme (e.g. Ubc13-Uev1a, ube2w, or UbcH5a/b/c) (16, 17). Most importantly, our study (which includes mutational studies) identified the key amino acids in BNIP-H that are involved in its ubiquitination by CHIP E3 ligase. While these exact mutations are not observed in Cayman ataxia patients, the mechanism of regulation of BNIP by CHIP ubiquitination is relevant as it dictates the functional BNIP-H population. This provides a starting point for understanding the molecular basis of Cayman ataxia, jittery movements, dystonia, and sidewinder phenotypes, which are currently understudied. Further, in the case of the CHIP E3 ligase, it is complicated by its interplay with dimerization, co-chaperone interaction and activity (9, 15, 17, 20, 34), which requires further investigation, especially in relation to BNIP-H.

The CHIP E3 ligase is involved in a wide range of functions, including protein folding, cell cycle regulation, and oncogenic transformations (9, 10, 26, 34–38). It plays an indispensable role in ubiquitinating substrates critical for neuronal function, such as tau protein, alpha-synuclein, and ataxin-3. The abnormal accumulation of any of these proteins can lead to neurodegenerative diseases (10, 19, 23). Although there is considerable understanding of the ubiquitin linkages borne by CHIP and its substrates, such as K63- or K48-linked ubiquitin chains (15, 20, 31), the specific details regarding BNIP-H remain to be elucidated. The BCH domain of BNIP-H likely attributes functional diversity and regulation as in the case of the yeast p50RhoGAP (ARHGAP1) where the β5-strand of the BCH domain is responsible for allosteric control of GAP activity (21). Moreover, further studies are required to highlight the importance of these lysine residues in context to BNIP-H mutants found in Cayman ataxia patients to provide a deeper understanding of the protein's role in neuronal physiology.

Material and methods

Cloning and site-directed mutagenesis

Genes for proteins of interest were inserted into the respective plasmids: UbcH5b, Ubiquitin, and CHIP into pGEX-6P-1; BNIP-H into pCDFDuet-1; UbE1 into pET21d. Site-directed mutagenesis was performed with polymerase chain reaction using Bioer BYQ6615 Thermal Cycler. Appropriate primers were designed and synthesized by Integrated DNA Technologies for the mutations. 0.7% agarose gel was used to confirm amplification. The amplicons were digested using New England Biolabs DpnI restriction enzyme and transformed into *Escherichia coli* strain DH5α cells. Plasmids were extracted using Bio Basic EZ-10 Spin Column Plasmid DNA Miniprep Kit and sequence analyzed with Bio Basic sequencing service.

Protein expression and purification

Confirmed plasmids were transformed into *E. coli* strain BL21 *via* heat shock. BL21 cells were grown in Bio Basic LB Broth Powder, Miller (SD7002) with respective plasmid-specific antibiotics: 0.10 g/mL Ampicillin (Sodium) for pGEX-6P-1 and pET21d, 0.05 g/mL Streptomycin for pCDFDuet-1. The *E. coli* was grown at 37 °C at 200 rpm until 0.6–0.8 optical density before being induced with 0.4 mM β-d-1-thiogalactopyranoside overnight at 16 °C at 120 rpm. The cultures were pelleted and washed with

1× phosphate-buffered saline (PBS) and kept at −20 °C until purification.

The pellets were resuspended in their respective lysis buffers containing optimized concentration of Tris, NaCl, glycerol, and DTT. In per 100 mL of resuspended pellet, one tablet of Sigma-Aldrich cOmplete, EDTA-free Protease Inhibitor Cocktail was dissolved. The cells were lysed, on ice, with a Sonics Vibra-Cell Sonicator. The lysate was passed through, depending on the tag, nickel or Glutathione S-transferase (GST) affinity columns. For the nickel beads, the proteins were eluted with 150, 300, and 500 mM imidazole (pH 7.4) while purified PreScission Protease was used to elute the GST-tagged proteins. The eluted proteins were further purified using ion-exchange and/or gel filtration chromatography, in optimized buffers, with an ÄKTA pure fast protein liquid chromatography machine. IEX chromatography was performed using GE Healthcare's Mono Q 5/50 GL or HiTrap Q HP (desalted with HiPrep 26/10). After IEX chromatography, a gel filtration chromatography was performed with HiLoad 16/600 Superdex 200 pg, HiLoad 16/600 Superdex 75 pg, Superdex 200 10/300 or Superdex 75 10/300 GL. Proteins were concentrated using Sartorius centricons into appropriate concentrations, flash-frozen with liquid N_2 and kept at −80 °C.

Ubiquitination assay

In vitro ubiquitination assays were performed on BNIP-H. According to their individual concentrations, appropriate molarities of UbE1 (0.3 μM), UbcH5b (10 μM), CHIP (2 μM), Ubiquitin (10 μM), BNIP-H (3 μM), ATP (4.5 mM), DTT (1 mM), and ubiquitination buffer (5 μL) were topped up to 50 μL with Milli-Q water. The Ubiquitination buffer consists of 50 mM Hepes pH 7.5, 100 mM NaCl, and 10 mM $MgCl_2$. Reaction samples without certain components were topped up with Milli-Q water. All reaction samples were incubated at 37 °C for 2 h at 500 rpm. To stop the reaction, 10 μL of 6× SDS loading dye was added and samples were heated at 100 °C for 3 min. Further analysis was performed with SDS-PAGE or western blots. ImageJ was used for the quantification of gel bands and analysis of differences in the ubiquitination patterns (39).

Western blot

Ubiquitination assay samples were run for SDS-PAGE by loading 5 μL per lane. The SDS gels were then transferred onto GE Healthcare's Amersham Hybond P 0.45 PVDF membranes using a Bio-Rad Trans-Blot Turbo Transfer System for 7–17 min (depending on optimization). The membranes were blocked at room temperature (~25 °C) for 1 h with rocking with 5% Bovine serum albumin in 1× PBS, 0.1% Tween 20 Detergent (PBST). The membranes were washed with 1× PBST with rocking and added with appropriate primary antibodies for 1 h binding. Primary antibodies used were: Santa Cruz Biotechnology's Ub Antibody (P4D1): sc-8017, CHIP Antibody (C-10): sc-133083, and BNIP-H Antibody: MBS6001808. After primary antibody binding, the membranes were washed, and appropriate Horseradish peroxidase (HRP)-conjugated secondary antibodies were added. Secondary antibodies were used, depending on the primary antibodies: GeneTex Goat Anti-Mouse IgG antibody (GTX213111-01) or Bethyl Rabbit IgG-heavy and light chain Antibody, A120-101P. Immobilon Crescendo HRP substrate was added to the membrane and incubated for 2–5 min. The membranes were imaged using a Syngene PXi fluorescence imager.

MS analysis of excised bands from in vitro ubiquitination assays

In-gel digestion

The gel band was cut into small pieces (1 mm^3). The finely cut pieces of gel were placed in a Sep-Pak tC18 96-well μElution Plate (Waters, Miltford, MA, USA). The gels were then washed with 50 mM ammonium bicarbonate/50% ethanol (v/v) and dehydrated using 100% ethanol, and the step was repeated one more time. Subsequently, samples were reduced with 10 mM dithiothreitol at 56 °C for 60 min followed by alkylation with 55 mM iodoacetamide for 60 min, in the dark, at room temperature. Following reduction and alkylation, the gel pieces were washed with 200 μL of 50 mM ammonium bicarbonate (for 30 min), 200 μL of 25 mM ammonium bicarbonate/5% acetonitrile (ACN) (for 30 min), 200 μL of 25 mM ammonium bicarbonate/50% ACN (for 30 min). Then the gel pieces were dehydrated by adding 200 μL of ACN for 10 min. One μg of trypsin per 20 μg of proteins was added, and trypsin digestion was performed at 37 °C for 18 h. The gels were then washed with 0.2% trifluoroacetic acid (TFA). The digested peptides were extracted with 70% ACN, 0.1% TFA.

LC–MS/MS analysis

The peptide separation was carried out on an Eksigent nanolC Ultra and ChiPLC-nanoflex (Eksigent) in trap-elute configuration. The samples were desalted with Sep-Pak tC18 μElution Plate (Waters) and reconstituted with 20 μL of diluent (98% Water, 2% ACN, 0.05% Formic acid [FA]). In total, 5 μL of the sample was loaded on a 200 μm × 0.5 mm trap column and separated on an analytical 75 μm × 150 mm column. Both trap and analytical columns were made of ChromXP C18-CL, 3 μm (Eksigent). Peptides were separated by a gradient formed by 2% ACN, 0.1% FA (mobile phase A) and 98% ACN, 0.1% FA (mobile phase B): 5 to 30% of mobile phase B in 10 min, 30 to 60% of mobile phase B in 4 min, 60 to 90% of mobile phase B in 1 min, 90 to 90% of mobile phase B in 5 min, 90 to 5% of mobile phase B in 1 min, and 5 to 5% of mobile phase B in 9 min, at a flow rate of 300 nL/min. The peptides eluted were detected and identified using SCIEX 5600 Triple ToF mass spectrometer using Analyst acquisition software.

Peptide identification and quantification was carried on the ProteinPilot 5.0.2 software Rev. 5346 (SCIEX) using the Paragon database search algorithm (5.0.20.5174) and the integrated false discovery rate (FDR) analysis function. The data were searched against a SWISSPROT *Mus musculus* database. The search parameters are as follows: Sample Type—Identification; Cys Alkylation—Iodoacetamide; Digestion—trypsin; Special Factors—Gel-based ID/Ubiquitin/SUMO enrichment; Species—None. The processing was specified as follows: ID Focus—Biological Modifications; Search Effort—Thorough; Detected Protein Threshold—0.05 (10.0%). For FDR determination, data were searched against a concatenated database with in silico on-the-fly reversal for decoy sequences automatically by the software. Only proteins with ≤1% global FDR and distinct peptides with ≤5% local FDR were used for further analysis.

Circular dichroism

Proteins performed with CD were concentrated to desired concentrations, based on preliminary optimization. Before measurement, the proteins were spun down at maximum speed for 7 min at 4 °C. The CD was performed using a JASCO J-1100 CD spectrophotometer. The cuvette was washed with 25% HNO_3 and Milli-Q water. The results were generated with JASCO

Spectra Manager. Baseline measurement was done with Milli-Q water. Data were processed in Microsoft Excel and K2D3 tool (41).

Isothermal titration calorimetry

The interaction between purified TPR domain from kinesin light chain (the domain is structurally similar to CHIP TPR domain) and the ^{112}NGNELEWEDDTP^{123} peptide from BNIP-H was characterized by MicroCal iTC200 system from Malvern. Here, 10 μM of protein was used in the sample cell, and the titrations were done using 220 μM peptide (purchased from GL Biochem Ltd). Prior to injection, the samples were degassed and centrifuged to clarify the protein. In addition, 4 μL volume of peptide per injection were used for the experiment, and each injection was separated by 4 min to allow the peak to return to baseline. Origin MicroCal iTC200 software was used to analyze the data.

HDX-MS experiments

Purified CHIP^{WT} and BNIP^{WT} proteins, 75 pmol each, were diluted in PBS (pD 7.4) prepared in deuterium oxide, to initiate the hydrogen–deuterium exchange. The H-to-D labeling reactions were carried out at 25 °C and incubated for predefined timepoints of 1, 10, and 100 min. The reaction was quenched by lowering the pD ~2.5 using chilled solution (0.75 M Guanidinium-HCl and 0.06% Trifluoro Acetic acid). Nondeuterated control experiments of CHIP^{WT} and BNIP^{WT} were performed using aqueous PBS. For CHIP^{WT}/BNIP^{WT} complex, the two proteins were mixed in 1:1 molar ratio and incubated for 30 min at 25 °C prior to each labeling experiment. Similarly, HDX-MS experiments were performed for purified CHIP^{9M} and BNIP-H^{4M} proteins and preincubated CHIP^{9M}/BNIP-H^{4M} complex.

HDX-MS experiments were analyzed using a nanoAcquity UPLC M-class system platform (Waters, Manchester, UK) equipped with an Enzymate BEH pepsin column, 2.1 × 30 mm (Waters, Milford, MA) for proteolysis, followed by ACQUITY UPLC BEH C18 1.7 μm VanGuard Pre-Column, 2.1 × 5 mm connected to ACQUITY UPLC BEH C18 1.7 μm, 1.0 × 100 mm analytical column (Waters, Milford, MA) as described previously (40–43). Protein digestion was performed at 12 °C, while chromatographic separation was carried out 3 °C to minimize back-exchange. The eluted peptides were detected using Synapt G2-Si mass spectrometer (Waters, UK) via electrospray ionization source. The mass spectrometer was operated in positive-ion mobility (HDMSe) mode. The peptides were identified using ProteinLynx Global Server (PLGS v3.0, Waters) using appropriate amino acid sequences of CHIP and BNIP-H proteins (WT and mutants). All deuterium exchange data were processed and analyzed using DynamX software v3.0 (Waters), with additional manual verification of the raw spectra. The parameters for peptide search and deuterium uptake assignment are as described previously (43, 44). Each deuterium exchange value reported is an average from biological ($n = 2$) and technical ($n = 3$) replicate measurements, and not corrected for back exchange. The differences in deuterium exchange are visualized as difference plots, and 1 min labeling data were mapped onto full-length models of the two proteins. HDX-MS metadata of the deuterium exchange of WT and mutant forms of CHIP and BNIP-H are tabulated in the Supplementary Material.

Supplementary Material

Supplementary material is available at *PNAS Nexus* online.

Funding

This work was supported by a Ministry of Education, Singapore, Tier 2 grant WBS No. A-8001519-00-00 and MoE Tier 1 grant WBS No. A-8000477-00-00. S.S. was a graduate scholar in receipt of a NUS research scholarship from the National University of Singapore (NUS).

Author Contributions

J.S. received funding and supervised the project. S.S. and J.S. designed the research. S.S., Y.L., and N.K.T. performed the research. S.S., Y.L., N.K.T., and J.S. analyzed the data. Q.L. supervised the MS experiments. B.C.L. helped in analyzing the data. S.S. and J.S. wrote the paper with inputs from all authors.

Data Availability

HDX-MS data (search files, raw, and processed data) have been uploaded onto ProteomeXchange Consortium server with identifier PXD: PXD054896. All other data are included in the manuscript and/or Supplementary Material.

Consent for Publication

All authors consent to publication of this work. The manuscript is original, has not already been published, and is not currently under consideration by another journal.

References

1 Boyd JM, *et al.* 1994. Adenovirus E1B 19 kDa and Bcl-2 proteins interact with a common set of cellular proteins. *Cell*. 79(2):341–351.
2 Bomar JM, *et al.* 2003. Mutations in a novel gene encoding a CRAL-TRIO domain cause human Cayman ataxia and ataxia/dystonia in the jittery mouse. *Nat Genet*. 35(3):264–269.
3 Sun J, *et al.* 2015. BNIP-H Recruits the cholinergic machinery to neurite terminals to promote acetylcholine signaling and neuritogenesis. *Dev Cell*. 34(5):555–568.
4 Buschdorf JP, *et al.* 2006. Brain-specific BNIP-2-homology protein Caytaxin relocalises glutaminase to neurite terminals and reduces glutamate levels. *J Cell Sci*. 119(16):3337–3350.
5 Aoyama T, *et al.* 2009. Cayman ataxia protein caytaxin is transported by kinesin along neurites through binding to kinesin light chains. *J Cell Sci*. 122(22):4177–4185.
6 Grelle G, *et al.* 2006. Identification of VCP/p97, carboxyl terminus of Hsp70-interacting protein (CHIP), and amphiphysin II interaction partners using membrane-based human proteome arrays*. *Mol Cell Proteomics*. 5(2):234–244.
7 Hershko A, Ciechanover A. 1998. THE ubiquitin system. *Annu Rev Biochem*. 67:425–479.
8 Ciechanover A, Schwartz AL. 1998. The ubiquitin-proteasome pathway: the complexity and myriad functions of proteins death. *Proc Natl Acad Sci U S A*. 95(6):2727–2730.
9 Murata S, Minami Y, Minami M, Chiba T, Tanaka K. 2001. CHIP is a chaperone-dependent E3 ligase that ubiquitylates unfolded protein. *EMBO Rep*. 2(12):1133.
10 Zhang S, Hu Z-W, Mao C-Y, Shi C-H, Xu Y-M. 2020. CHIP as a therapeutic target for neurological diseases. *Cell Death Dis*. 11(9):727.
11 Guo Y, *et al.* 2019. Degradation of caytaxin causes learning and memory deficits via activation of DAPK1 in aging. *Mol Neurobiol*. 56(5):3368–3379.

12 Jiang J, *et al.* 2001. CHIP is a U-box-dependent E3 ubiquitin ligase: identification of Hsc70 as a target for ubiquitylation. *J Biol Chem*. 276(46):42938–42944.

13 Kuznetsova KG, *et al.* 2021. Cysteine alkylation methods in shotgun proteomics and their possible effects on methionine residues. *J Proteomics*. 231:104022.

14 Kuznetsova KG, Solovyeva EM, Kuzikov AV, Gorshkov MV, Moshkovskii SA. 2020. Modification of cysteine residues for mass spectrometry-based proteomic analysis: facts and artifacts. *Biomed Khim*. 66(1):18–29.

15 Nielsen ML, *et al.* 2008. Iodoacetamide-induced artifact mimics ubiquitination in mass spectrometry. *Nat Methods*. 5(6):459–460.

16 Windheim M, Peggie M, Cohen P. 2008. Two different classes of E2 ubiquitin-conjugating enzymes are required for the mono-ubiquitination of proteins and elongation by polyubiquitin chains with a specific topology. *Biochem J*. 409(3):723–729.

17 Balaji V, *et al.* 2022. A dimer-monomer switch controls CHIP-dependent substrate ubiquitylation and processing. *Mol Cell*. 82(17):3239–3254.e11.

18 Scaglione KM, *et al.* 2013. The ubiquitin-conjugating enzyme (E2) ube2w ubiquitinates the N terminus of substrates. *J Biol Chem*. 288(26):18784–18788.

19 Scaglione KM, *et al.* 2011. Ube2w and Ataxin-3 coordinately regulate the ubiquitin ligase CHIP. *Mol Cell*. 43(4):599–612.

20 Zhang M, *et al.* 2005. Chaperoned ubiquitylation-crystal structures of the CHIP U box E3 ubiquitin ligase and a CHIP-Ubc13-Uev1a complex. *Mol Cell*. 20:525–538.

21 Chichili VPR, Chew TW, Shankar S, Er SY, Chin CF, *et al.* 2021. Structural basis for p50RhoGAP BCH domain-mediated regulation of Rho inactivation. *Proc Natl Acad Sci U S A*. 118(21): e2014242118.

22 Shankar S, Chew TW, Chichili VPR, Low BC, Sivaraman J. 2024. Structural basis for the distinct roles of non-conserved Pro116 and conserved Tyr124 of BCH domain of yeast p50RhoGAP. *Cell Mol Life Sci*. 81(1):216.

23 Joshi V, *et al.* 2016. A decade of boon or burden: what has the CHIP ever done for cellular protein quality control mechanism implicated in neurodegeneration and aging? *Front Mol Neurosci*. 9:93.

24 Liwocha J, *et al.* 2021. Linkage-specific ubiquitin chain formation depends on a lysine hydrocarbon ruler. *Nat Chem Biol*. 17(3):272–279.

25 Middleton AJ, Day CL. 2015. The molecular basis of lysine 48 ubiquitin chain synthesis by Ube2K. *Sci Rep*. 5(1):16793.

26 Murata S, Chiba T, Tanaka K. 2003. CHIP: a quality-control E3 ligase collaborating with molecular chaperones. *Int J Biochem Cell Biol*. 35:572–578.

27 Wang L, *et al.* 2011. Molecular mechanism of the negative regulation of smad1/5 protein by carboxyl terminus of Hsc70-interacting protein (CHIP). *J Biol Chem*. 286(18):15883–15894.

28 Taylor CA, Miller BR, Shah SS, Parish CA. 2017. A molecular dynamics study of the binary complexes of APP, JIP1, and the cargo binding domain of KLC. *Proteins: Struct, Funct Bioinf*. 85(2):221–234.

29 Pernigo S, *et al.* 2018. Structural basis for isoform-specific kinesin-1 recognition of Y-acidic cargo adaptors. *Elife*. 7:e38362.

30 Jiang YH, Beaudet AL. 2004. Human disorders of ubiquitination and proteasomal degradation. *Curr Opin Pediatr*. 16(4):419–426.

31 Tatham MH, *et al.* 2013. Ube2W conjugates ubiquitin to α-amino groups of protein N-termini. *Biochem J*. 453:137–145.

32 Lam YA, Xu W, DeMartino GN, Cohen RE. 1997. Editing of ubiquitin conjugates by an isopeptidase in the 26S proteasome. *Nature*. 385(6618):737–740.

33 Thrower JS, Hoffman L, Rechsteiner M, Pickart CM. 2000. Recognition of the polyubiquitin proteolytic signal. *EMBO J*. 19(1):94–102.

34 Shimura H, Schwartz D, Gygi SP, Kosik KS. 2004. CHIP-Hsc70 Complex ubiquitinates phosphorylated tau and enhances cell survival*. *J Biol Chem*. 279(6):4869–4876.

35 Paul I, Ghosh MK. 2014. The E3 ligase CHIP: insights into its structure and regulation. *Biomed Res Int*. 2014:918183.

36 Shang Y, *et al.* 2017. CHIP/stub1 regulates the Warburg effect by promoting degradation of PKM2 in ovarian carcinoma. *Oncogene*. 36:4191–4200.

37 Seo J, *et al.* 2018. K6 linked polyubiquitylation of FADD by CHIP prevents death inducing signaling complex formation suppressing cell death. *Oncogene*. 37:4994–5006.

38 Xu J, *et al.* 2018. CHIP functions as an oncogene by promoting colorectal cancer metastasis via activation of MAPK and AKT signaling and suppression of E-cadherin. *J Transl Med*. 16:169.

39 Schneider CA, Rasband WS, Eliceiri KW. 2012. NIH image to ImageJ: 25 years of image analysis. *Nat Methods*. 9(7):671–675.

40 Wales TE, Fadgen KE, Gerhardt GC, Engen JR. 2008. High-Speed and high-resolution UPLC separation at zero degrees celsius. *Anal Chem*. 80(17):6815–6820.

41 Louis-Jeune C, Andrade-Navarro MA, Perez-Iratxeta C. 2012. Prediction of protein secondary structure from circular dichroism using theoretically derived spectra. *Proteins*. 80(2):374–455.

42 Guttman M, *et al.* 2016. Tuning a high transmission Ion guide to prevent gas-phase proton exchange during H/D exchange MS analysis. *J Am Soc Mass Spectrom*. 27(4):662–668.

43 Tulsian NK, Ghode A, Anand GS. 2020. Adenylate control in cAMP signaling: implications for adaptation in signalosomes. *Biochem J*. 477(16):2981–2998.

44 Yadav M, *et al.* 2021. Binding specificity of type three secretion system effector NleH2 to multi-cargo chaperone CesT and their phosphorylation. *Protein Sci*. 30(12):2433–2444.